



**HAL**  
open science

# SAR Image Segmentation via Non-local Active Contours

Gang Liu, Gui-Song Xia, Wen Yang

► **To cite this version:**

Gang Liu, Gui-Song Xia, Wen Yang. SAR Image Segmentation via Non-local Active Contours. 2013.  
hal-00839601

**HAL Id: hal-00839601**

**<https://hal.science/hal-00839601>**

Submitted on 13 Jan 2014

**HAL** is a multi-disciplinary open access archive for the deposit and dissemination of scientific research documents, whether they are published or not. The documents may come from teaching and research institutions in France or abroad, or from public or private research centers.

L'archive ouverte pluridisciplinaire **HAL**, est destinée au dépôt et à la diffusion de documents scientifiques de niveau recherche, publiés ou non, émanant des établissements d'enseignement et de recherche français ou étrangers, des laboratoires publics ou privés.

# SAR IMAGE SEGMENTATION VIA NON-LOCAL ACTIVE CONTOURS

Gang Liu<sup>1,2</sup>, Zifeng Wang<sup>1</sup>, Gui-Song Xia<sup>1</sup>, Wen Yang<sup>2</sup>

<sup>1</sup> Key State Laboratory LIESMARS, Wuhan University, Wuhan 430079, China

<sup>2</sup> Signal Processing Lab, Electronics Information School, Wuhan University, Wuhan, 430079, China

## ABSTRACT

This paper presents a method for SAR image segmentation by relying on active contour model with the non-local processing principle [1]. The idea is to partition a SAR image via computing the patch similarity in the SAR image non-locally, and formalize the segmentation problem with an active contour model. More precisely, after computing the statistical features of SAR images, non-local comparisons between feature patches are used to calculate the active contour energy, which is defined by integrating the interactions between pairs of patches inside and outside the segmented region. A level set method is finally used to minimize the non-local energy. Compared with existing approaches for SAR image segmentation, the only requirement of this method is a local similarity between patches, and it is less sensitive to initial segmentation. The experimental results show the effectiveness and feasibility of the proposed method.

## 1. INTRODUCTION

Synthetic aperture radar (SAR) systems have been widely used in remote-sensing application for many years due to its advantage of strong penetrability and all-weather acquisition capability. As one of the fundamental problems to understand SAR data, the segmentation of SAR images is challenging because of the speckle effects, which can be described by a multiplicative noise model. This problem has been widely investigated in the literature [2, 3], among which active contour models show many advantages.

The early works on this topic include the method proposed by Germain *et al.* [4], where in order to segment a SAR image, a likelihood ratio edge detector has been employed to localize the edges of the image and refine them subsequently with the “snake model” [5] for achieving the final result. Instead of evolving discretized curves, level set functions has been proposed to solve the active contour models [6]. The extension of this method to SAR image segmentation includes [7]. Recently, in order to get a better segmentation of SAR images, the energy function was modified to achieve a stationary global minimum of the optimization problem [8]. In [9], the Kullback-Leibler divergence of Edgeworth was used instead to segment SAR images into homogeneous regions accurately. In [10], a multi-scale level set

approach was proposed for segmenting SAR images. However, these methods impose a global homogeneity to a SAR image, meaning that the SAR image inside and outside the regions to be segmented are homogeneous respectively, which are usually not true for SAR images and the results are heavily affected by speckles.

To overcome this problem, this paper proposes to use the non-local active contour model [11] for SAR image segmentation, which only requires a local homogeneity to the image, in contrast to other methods. In particular, a non-local energy is defined by using a pairwise interaction of features inside and outside the regions to be segmented. In our context, the pairwise interaction is calculated by evaluating the patch similarity in a non-local way [1]. More precisely, each patch is described by a logarithmic normal distributions and the patch similarity is measured by the Kullback-Leibler divergence between the distributions. As we shall see, this method is robust to speckles in SAR images.

The remainder of this paper is organized as follows. In section II, we present the non-local active contour model for SAR image segmentation. In section III, we show the experimental results and conclude the paper in section IV.

## 2. A NON-LOCAL ACTIVE CONTOUR MODEL FOR SAR IMAGE SEGMENTATION

In this section, we formalize the SAR image segmentation problem via non-local active contours.

### 2.1. Non-local active contour model

Let  $f : \Omega \rightarrow R$  be an image, with  $\Omega$  as the image grid and  $\partial\Omega$  as its boundary. The patch  $p_s$  centered on  $s \in \Omega$  is denoted by  $p_s(k) = f(s+k)$ ,  $k \in \Omega_\tau = [-\tau/2, \tau/2]^2$ , with  $\tau$  to be the width of the patch. Let  $C$  be a curve in the image domain  $\Omega$  to partition the image  $f$  into two parts: part inside  $C$  and the part outside  $C$ . The basic idea of the non-local active contour model [11] for segmentation is to evolve the curve  $C$  that captures the objects of interest. With a level-set method, the curve  $C$  is represented by the zero cross of the level-set function  $\phi : \Omega \rightarrow R$ , *i.e.*  $C = \{s|\phi(s) = 0\}$ . The non-local active contour model computes the segmentation of an image

$f$  as a stationary point of the following optimization problem

$$\min_{\phi} E(\phi) + \gamma L(\phi) \quad (1)$$

where  $\phi$  is the level set function.  $E(\phi)$  is the the energy that measures the dissimilarity inside and outside the contour  $C$ .  $L(\phi)$  is a regularization term and  $\gamma$  is a weight parameter to balance the two terms.

The energy  $E(\phi)$  is computed in a non-local way as

$$\begin{aligned} E(\phi) = & \int \int_{S \times S} G_{\alpha}(s-t) \cdot d(p_s, p_t) ds dt \\ & + \int \int_{S^c \times S^c} G_{\alpha}(s-t) \cdot d(p_s, p_t) ds dt, \end{aligned} \quad (2)$$

where  $p_s$  and  $p_t$  are the patches centered on pixel  $s$  and  $t$  respectively.  $S$  and  $S^c$  denotes the regions inside and outside the contour  $C$  respectively, with  $S \cup S^c = \Omega$  and  $S \cap S^c = \emptyset$ .  $G_{\alpha}(\cdot)$  is a Gaussian kernel with the scale of  $\alpha$ . The first term of Eq.(2) measures the internal energy while the second term measures the external energy.

For simplicity, the integration inside and outside the contour  $C$  is implemented with a Heaviside function

$$H(u) = \frac{1}{2} + \frac{1}{\pi} \arctan\left(\frac{u}{\varepsilon}\right), \quad (3)$$

where the parameter  $\varepsilon$  should be small enough for a sharp boundary.

Combining Eq. (2) and Eq. (3), we have

$$\begin{aligned} E(\phi) = & \int \int \rho\left(H(\phi(s)), H(\phi(t))\right) \\ & \cdot G_{\alpha}(s-t) \cdot d(p_s, p_t) ds dt \end{aligned} \quad (4)$$

where  $\rho$  is the indicator function defined as  $\rho(u, v) = 1 - |u - v|$ , implying that only pairs of pixels for which  $\phi$  has the same sign are considered.

The segmentation region is penalized by the length of the contour  $C$  as

$$L(\phi) = \int \|\nabla H(\phi(s))\| ds. \quad (5)$$

Combining Eq. (1), Eq. (4) and Eq. (5), one can obtain the optimization function, the minimization of which can be achieved by using an iterative scheme proposed in [11].

## 2.2. Pairwise patch interaction

The left problem is how to compute the pairwise patch interactions in the context of segmenting SAR images. The pairwise patch similarities has been recently investigated by Deledalle *et al.* [12], which shows that the statistical distribution characteristics perform the best among others on SAR images.

There are many probabilistic distribution functions available to describe SAR images, such as the logarithmic normal distribution, Rayleigh distribution, Gamma distribution, K distribution,  $G_A^0$  distribution, *etc* [13]. Though the logarithmic normal distribution is a simple statistical model for SAR images, our experiments show that it is efficient enough for many SAR image segmentation in our context.

The pixels in image patches are described by the logarithmic normal distribution [13], defined as

$$g(z) = \frac{1}{\sqrt{2\pi}\sigma z} \exp\left(-\frac{(\ln z - \mu)^2}{2\sigma^2}\right), \quad (6)$$

where  $z$  is the intensity of the pixels,  $\mu$  and  $\sigma$  are the average and the variance of the logarithmic image patch respectively.

After the parameter  $\mu$  and  $\sigma$  of each patch are estimated, the distribution of pixels in the patch could be obtained by Eq. (6).

Given two patches  $p_s$  and  $p_t$  centered on  $s, t \in \Omega$ , the Kullback-Leibler divergence between them is implemented as

$$d(p_s, p_t) = \int g_s(z) \cdot \log \frac{g_s(z)}{g_t(z)} dz, \quad (7)$$

where  $g_s(z)$  and  $g_t(z)$  denote logarithmic normal distributions, the features of the patch  $p_s$  and  $p_t$  respectively. Considering the dissymmetry of  $d(p_s, p_t)$  and  $d(p_t, p_s)$ , we rewrite Eq. (7) by

$$\begin{aligned} d(p_s, p_t) = & \int g_s(z) \cdot \log \frac{g_s(z)}{g_t(z)} dz \\ & + \int g_t(z) \cdot \log \frac{g_t(z)}{g_s(z)} dz, \end{aligned} \quad (8)$$

From Eq.(6) and Eq.(8), we have

$$d(p_s, p_t) = \frac{1}{2} \left( \frac{\sigma_s^2}{\sigma_t^2} + \frac{\sigma_t^2}{\sigma_s^2} \right) + \frac{(\mu_s - \mu_t)^2}{2} \cdot \left( \frac{1}{\sigma_s^2 + \sigma_t^2} \right), \quad (9)$$

where  $\mu_s$  and  $\mu_t$  ( $\sigma_s$  and  $\sigma_t$  resp.) are the average (standard derivation resp.) of the logarithmic image patches  $\log p_s$  and  $\log p_t$ . This divergence is close to zero if the two patches are similar, and it is large if the two patches are dissimilar.

## 3. EXPERIMENTAL RESULTS

This section evaluates the proposed method on three kinds of real SAR images. The first includes three MSTAR SAR images of tanks. The second is an X-band Cosmo-Skymed SAR image with a spatial resolution of 3m. The last one is a C-band ENVISAT SAR image with a spatial resolution of 30m. The proposed method is compared with that in [8].

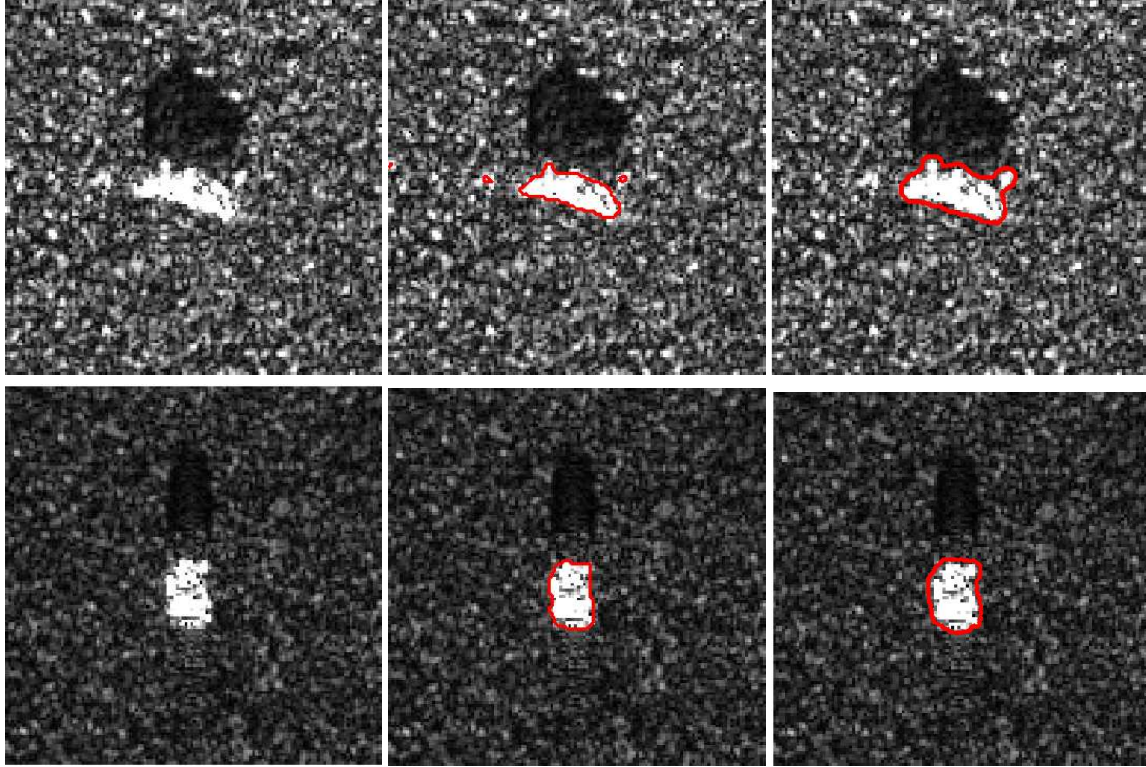


Fig. 1. Results on three MSTAR SAR images. From left to right: the original images, the results of [8] and our results.

### 3.1. MSTAR tank extraction

This experiment tests the proposed method on three MSTAR SAR images for tank extraction. The patch width  $\tau$  is set to be 5 and the non-local region width  $q$  is set to be 51. Thus,  $\gamma$  is set to be  $\frac{5}{n \times q^2 \times \tau^2} = \frac{1}{13005n}$ , with  $n$  as the number of pixels in images. The evolution of the contour is not sensitive to the initialization, and usually converges to the boundary of the object after about 50 iterations. Fig. 1 shows the results of MSTAR SAR images. The left column displays the original images, the middle column shows the segmentation results of the method in [8] and the right column illustrates the results of the proposed approach. We can see that in the results of [8], some small regions are segmented to be objects due to speckles, while the proposed method extracts out the tanks excellently and are more robust to speckle. This is mainly because we use the similarity of patches instead of pixels.

### 3.2. Pond extraction

In this experiment, a  $500 \times 500$  Cosmo-Skymed SAR image which contains a pond is used to validate the proposed method. The patch size  $\tau$  is set to be 9. The non-local region size  $q$  is set to be 101.  $\gamma$  is set to  $\frac{5}{n \times q^2 \times \tau^2}$ , with  $n$  as the number of pixels in images. The results are shown in Fig. 2. The left column shows the original image of a pond, the middle

column displays the segmentation result of [8] and the right column provides our result. In the segmentation result of [8], a lot of small regions in the homogenous areas are segmented to be object. However, in our result, the pond are detected out successfully.

### 3.3. Oil spill extraction

The proposed method is also tested on a  $500 \times 500$  ENVISAT ASAR image which contains oil spills. We use the same parameter settings as for the Experiment B. Fig. 2 illustrates the results. The left column gives the original SAR image of oil spill, the middle column displays the segmentation result of [8], and the right column shows our result. In the segmentation result of [8], many regions in oil spill are not extracted but our method gives much better result, which proves that the proposed method is promising to for the oil spill detection problem.

## 4. CONCLUSION

This paper has presented a method of SAR image segmentation via non-local active contour which is focusing on the feature of patches and the metric of similarity of patches in SAR images. The experimental results show that proper feature and metric of similarity are very important in SAR im-

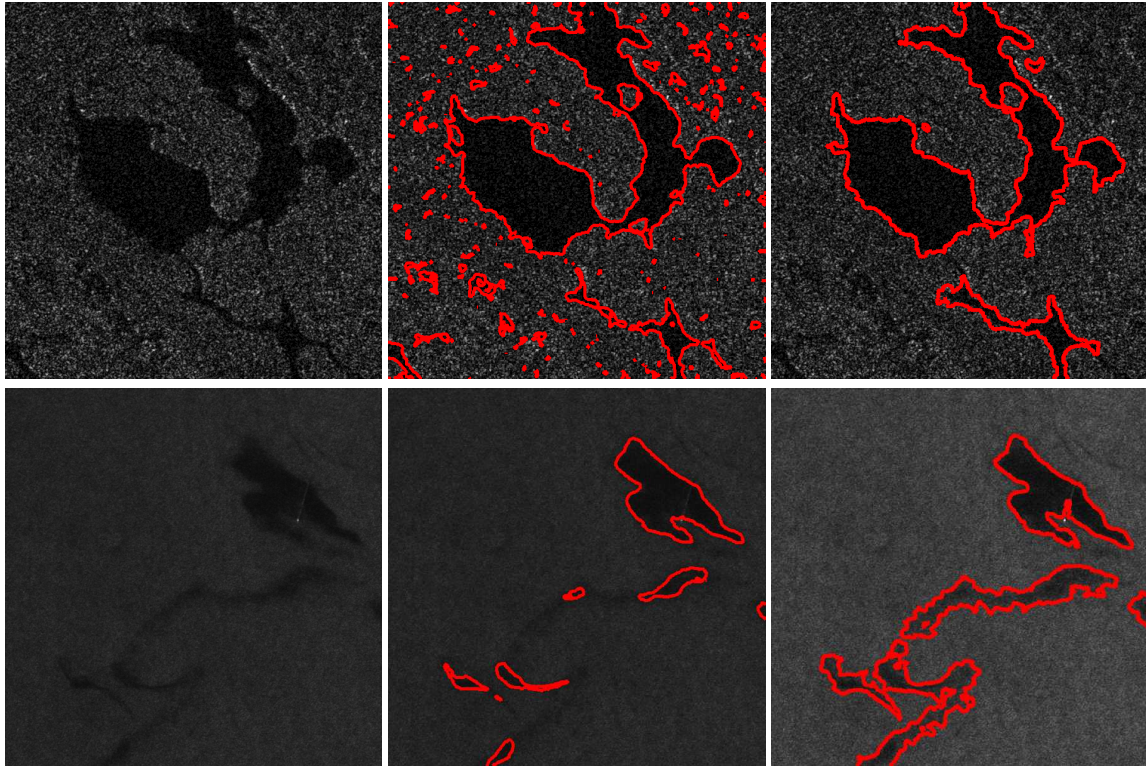


**Fig. 2.** Segmenting SAR images of a pond (top) and oil spill (bottom). From left to right: original image, result of [8] and our result.

ages segmentation. In the future work, we will extend the proposed method to multi-polarization SAR images.

## 5. REFERENCES

- [1] A. Buades, B. Coll, and J.-M. Morel, “Image denoising methods. a new nonlocal principle,” *SIAM review*, vol. 52, no. 1, pp. 113–147, 2010.
- [2] X.R. Zhang, L.C. Jiao, F. Liu, L.F. Bo, and M.G. Gong, “Spectral clustering ensemble applied to sar image segmentation,” *IEEE Trans. on Geoscience and Remote Sensing*, vol. 46, no. 7, pp. 2126–2136, 2008.
- [3] G.-S. Xia, C. He, and H. Sun, “A rapid and automatic mrf-based clustering method for sar images,” *IEEE Geoscience and Remote Sensing Letters*, vol. 4, no. 4, pp. 596–600, 2007.
- [4] O. Germain and P. Réfrégier, “Edge location in sar images: Performance of the likelihood ratio filter and accuracy improvement with an active contour approach,” *IEEE Trans. on Image Processing*, vol. 10, no. 1, pp. 72–78, 2001.
- [5] M. Kass, A. Witkin, and D. Terzopoulos, “Snakes: Active contour models,” *International Journal of Computer Vision*, vol. 1, no. 4, pp. 321–331, 1988.
- [6] S. Osher and J.A. Sethian, “Fronts propagating with curvature-dependent speed: algorithms based on hamilton-jacobi formulations,” *Journal of computational physics*, vol. 79, no. 1, pp. 12–49, 1988.
- [7] Ismail Ben Ayed, Student Member, , Ziad Belhadj, Amar Mitiche, and Ziad Belhadj, “Multiregion level-set partitioning of synthetic aperture radar images,” *IEEE Trans. on Pattern Analysis and Machine Intelligence*, vol. 27, pp. 793–800, 2005.
- [8] Y.M. Shuai, H. Sun, and G. Xu, “Sar image segmentation based on level set with stationary global minimum,” *IEEE Geoscience and Remote Sensing Letters*, vol. 5, no. 4, pp. 644–648, 2008.
- [9] L. Hu, Y. Ji, Y. Li, and F. Gao, “Sar image segmentation based on kullback-leibler distance of edgeworth,” in *Advances in Multimedia Information Processing-PCM 2010*, pp. 549–557. Springer, 2010.
- [10] H.G. Sui, C. Xu, J.Y. Liu, K.M. Sun, and C.F. Wen, “A novel multi-scale level set method for sar image segmentation based on a statistical model,” *International Journal of Remote Sensing*, vol. 33, no. 17, pp. 5600–5614, 2012.
- [11] M. Jung, G. Peyre, and L. D. Cohen, “Non-local active contours,” *SIAM J. Imaging Sciences*, vol. 5, no. 3, pp. 1022–1054, 2012.
- [12] C-A Deledalle, L. Denis, and Florence Tupin, “Iterative weighted maximum likelihood denoising with probabilistic patch-based weights,” *IEEE Trans. on Image Processing*, vol. 18, no. 12, pp. 2661–2672, 2009.
- [13] M. Soumekh, *Synthetic aperture radar signal processing*, Wiley New York, 1999.